Insight into Covalent Flavinylation and Catalysis from Redox, Spectral, and Kinetic Analyses of the R474K Mutant of the Flavoprotein Subunit of *p*-Cresol Methylhydroxylase[†]

Igor Efimov, Ciarán N. Cronin,[‡] David J. Bergmann,[§] Vladislav Kuusk,[||] and William S. McIntire*

Molecular Biology Division, Department of Veterans Affairs Medical Center, San Francisco, California 94121, and Department of Biochemistry and Biophysics, University of California, San Francisco, California 94143

Received October 1, 2003; Revised Manuscript Received March 12, 2004

ABSTRACT: Each flavoprotein subunit (PchF) of *p*-cresol methylhydroxylase (PCMH) has flavin adenine dinucleotide (FAD) covalently tethered to Tyr384. The PCMH structure suggests that Arg474 in PchF is required for self-catalytic covalent flavinylation and for substrate oxidation. The replacement of Arg474 with Lys was carried out to probe the subtleties of the role of Arg474 in these processes. In nearly all of the aspects examined, the mutant protein showed compromised properties relative to the wild-type protein, including the tenacity of noncovalent FAD binding to the apo-protein, the rate of covalent flavinylation, the affinity of the covalent flavoprotein for PchC (the cytochrome subunit), the k_{cat} for substrate oxidation, and the affinity for substrate analogues in the formation of FAD-charge-transfer complexes (CT complexes). Nevertheless, because the mutant retains these attributes, the comparison allows for an examination of the role of this residue in the various properties of the enzyme. A correlation is proposed to exist between ν_m, the frequency for the absorbance maximum of the CT complex with a substrate analogue, and k_{cat}, the steady-state rate constant for oxidation of *p*-cresol by various forms of PCMH and PchF; both ν_m and k_{cat} can be expressed as functions of the ionization potential of the donor (I^D) and the electron affinity of the acceptor (E^A). This correlation is a better predictor of the rate constant for substrate oxidation than is the magnitude of the redox potential, $E_{m,7}$, of the bound FAD, which was determined for the various mutant enzyme species and compared with those of the wild type.

The A form of *p*-cresol methylhydroxylase (PCMH;[1] EC 1.17.99.1) from *Pseudomonas putida* NCIMB 9869 (*1*) oxidizes *p*-cresol to 4-hydroxybenzyl alcohol, which is oxidized subsequently by this enzyme to produce 4-hydroxybenzaldehyde (*2*, *3*). PCMH has an $\alpha_2\beta_2$ structure consisting of a tightly associated homodimer of 59.5-kDa flavoprotein subunits (α_2 or $PchF_2$) and a monomeric 9.2-kDa *c*-type cytochrome subunit (β or PchC) bound to each α subunit (*4*−*6*). Although the cytochrome-free holo-$PchF_2$ catalyzes the oxidation of *p*-cresol, its k_{cat} value is only a few percent that of intact PCMH (*3*, *7*).

Flavin adenine dinucleotide (FAD) is covalently attached to each PchF subunit via an ether linkage between the 8α carbon of the isoalloxazine ring of flavin and the aromatic oxygen of Tyr384 (*8*, *9*) (Figure 1). Mere binding of PchC to PchF with FAD noncovalently bound ($PchF^{NC}$) induces a unique self-catalytic reaction for covalent flavinylation (*9*, *10*). Whereas covalent attachment of the FAD enhances electron transfer (ET) from the flavin to the heme (*6*, *9*), it is not essential for catalysis, because $PchF^{NC}$ rapidly oxidized 4-hydroxybenzyl alcohol and could oxidize *p*-cresol, albeit at a slower rate (*10*).

The X-ray crystallographic structures of native PCMH (PDB 1DII, Figure 2) and the PCMH•*p*-cresol complex (PDB 1DIQ, Figure 1) implicate a number of amino acyl residues within PchF that may play important roles in the covalent attachment of the FAD and in catalyzing substrate oxidation (*6*). One of these, Arg474, is part of the intricate hydrogen-bonding system (Figure 2). The guanidino N−H functionalities of Arg474 are hydrogen bonded directly to an active-

[†] This work was supported by the Department of Veterans Affairs and NIH Grant GM-61651.

* To whom correspondence should be addressed: The Molecular Biology Division (151-S), Department of Veterans Affairs Medical Center, San Francisco, CA 94121. Tel.: 415-387-1431. Fax: 415-650-6959. E-mail: wsm@itsa.ucsf.edu.

[‡] Present address: Pfizer Inc., 10777 Science Center Drive, San Diego, CA 92121.

[§] Present address: Department of Biochemistry, University of Minnesota, St. Paul, MN 55108.

[||] Present address: Logitech Inc., 6505 Kaiser Drive, Fremont, CA 94555.

[1] Abbreviations: 6-HDNO, 6-hydroxy-D-nictotine oxidase; BTP, BisTrisPropane, 1,3-bis[tris(hydroxymethyl)methylamino]propane; ^{C}, covalently bound FAD; CT and CTC, charge transfer and charge-transfer complex, respectively; DCIP, 2,6-dichlorophenol indophenol; ET, electron transfer; IEF, isoelectric focusing; KIE, kinetic isotope effect; OYE, old yellow enzyme; PCMH, *p*-cresol methylhydroxylase; ^{NC}, noncovalently bound FAD; PES, phenazine ethosulfate; PchC, *c*-type cytochrome subunit of PCMH; PchF, wild-type flavoprotein subunit of PCMH; $PchF^C$ and $PchF^{NC}$, wild-type flavoprotein subunit of PCMH with covalently bound and noncovalently bound FAD, respectively; PchF[Y384F], $PchF[Y384F]^{NC}$, and $PCMH[Y384F]^{NC}$, apo and holo forms of the Y384F variant of PchF, and PCMH with the Y384F variant of PchF; PchF[R474K], the R474K variant of apo-PchF; $PchF[R474K]^C$ and $PchF[R474K]^{NC}$, PchF[R474K] that contains covalently bound and noncovalently bound FAD, respectively; $PCMH[R474K]^C$, PCMH with the R474K variant of $PchF^C$; SDS, sodium dodecyl sulfate, PAGE, polyacrylamide gel electrophoresis; TMADH, trimethylamine dehydrogenase.

10.1021/bi035772x CCC: $27.50
Published on Web 04/27/2004

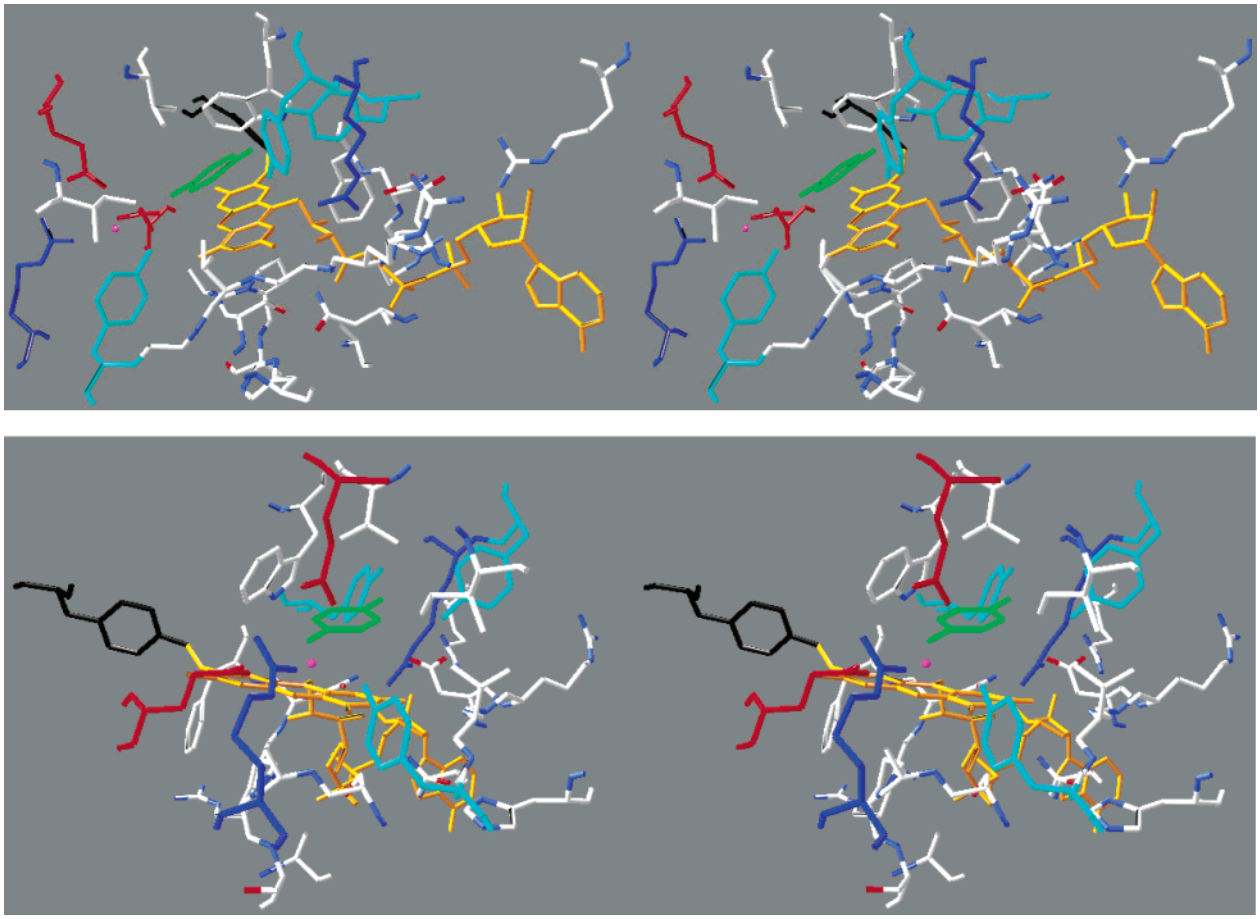

FIGURE 1: Stereoviews of the flavin/substrate binding site of PCMH. FAD is colored orange, and Tyr384 is colored black. Tyr384 is covalently attached, via an ether linkage, to the 8α carbon of the isoalloxazine ring of the flavin. Note that the methyl group (pointing to the left, top) of *p*-cresol(ate) (green) is positioned over the N5 position of the isoalloxazine ring of FAD. The methyl group is pointing toward the viewer in the bottom frame. Note also the orientation and distance between *p*-cresol and the isoalloxazine rings of the putative CTC. (Top) The aromatic OH groups of Tyr95 and Tyr473, colored cyan at the upper-middle part of the figure, hydrogen bond with the phenolate oxygen of *p*-cresol. Tyr172 (cyan), Arg368 (dark blue), Glu380, and Glu427 (both red), at the left in the figure, interact with a water molecule (small magenta sphere) that hydroxylates the quinone methide intermediate of oxidized *p*-cresol to produce 4-hydroxybenzyl alcohol. Arg474 is colored dark blue (upper-middle of the figure). Several hydrophobic and aromatic groups that interact with the benzene ring of *p*-cresol(ate) to position it appropriately in the active site are displayed also, as are a number of residues that are involved in the hydrogen-bonding network between groups of the isoalloxazine ring and ribityl side chain of the flavin and Arg474 (see Figure 2). The bottom displays the same structural elements rotated by ~90° about the *z* axis.

site water molecule, the *C2* oxygen of the isoalloxazine ring, and the 3′ oxygen of the ribityl side chain of FAD. Other amino acyl groups are also hydrogen bonded to these oxygens, the 4′ oxygen of the ribityl group, and the guanidino N−H functionalities of Arg474.

The positive charge on the side chain of Arg474 is considered to be essential for the covalent attachment of FAD to PchF (*9*−*11*) by stabilizing the negative charge on the *C2* oxygen of the anionic flavin iminoquinone methide-type intermediate (structure **II** in Figure 3), following the base removal of a proton from the 8α methyl carbon of the flavin. The phenolate oxygen of Tyr384 then attacks the electrophilic 8α methide carbon of the flavin to form two-electron-reduced FAD to yield covalently flavinylated PchF (*9*−*11*).

Our earlier studies (*12*) led us to conclude that the binding of PchC to $PchF^{NC}$ increases the potential of the FAD substantially, which likely results in an electrophilic activation of the 8α carbon of the isoalloxazine ring to increase the acidity of the hydrogens attached to this carbon. This would lead to a more facile formation of the iminoquinone methide (Step 1 in Figure 3), a prerequisite to nucleophilic attack on this intermediate by the phenolate oxygen of Tyr384 (Step 2 in Figure 3).

As a result of our past efforts, we have established that the covalent flavin linkage is multipurpose. First, it is part of the ET pathway from reduced FAD to the oxidized heme of PchC. Second, it stabilizes the association of PchC and $PchF^{C}$ in the $\alpha\beta$ heterodimeric unit of wild-type PCMH ($\beta\alpha$:$\alpha\beta$). Last, it significantly increases the potential of the bound FAD, which facilitates substrate oxidation (*12*). During catalysis, PCMH oxidation of the substrate presumably results in the formation of an anionic two-electron-reduced flavin (Figure 3A), in which case the negative charge on the *C2* oxygen of the fully reduced FAD is stabilized also by the positively charged guanidino group of Arg474 (*6*, *13*).

In this paper, the roles of Arg474 in PCMH are examined by studying the properties of a site-specific mutant form of PchF in which this Arg has been replaced by Lys (PchF-[R474K]). Recombinant PchF[R474K] produced by our *Escherichia coli* expression system, which does not produce PchC, contains noncovalently bound FAD, i.e., $PchF\text{-}[R474K]^{NC}$ that, when exposed to PchC, becomes covalently

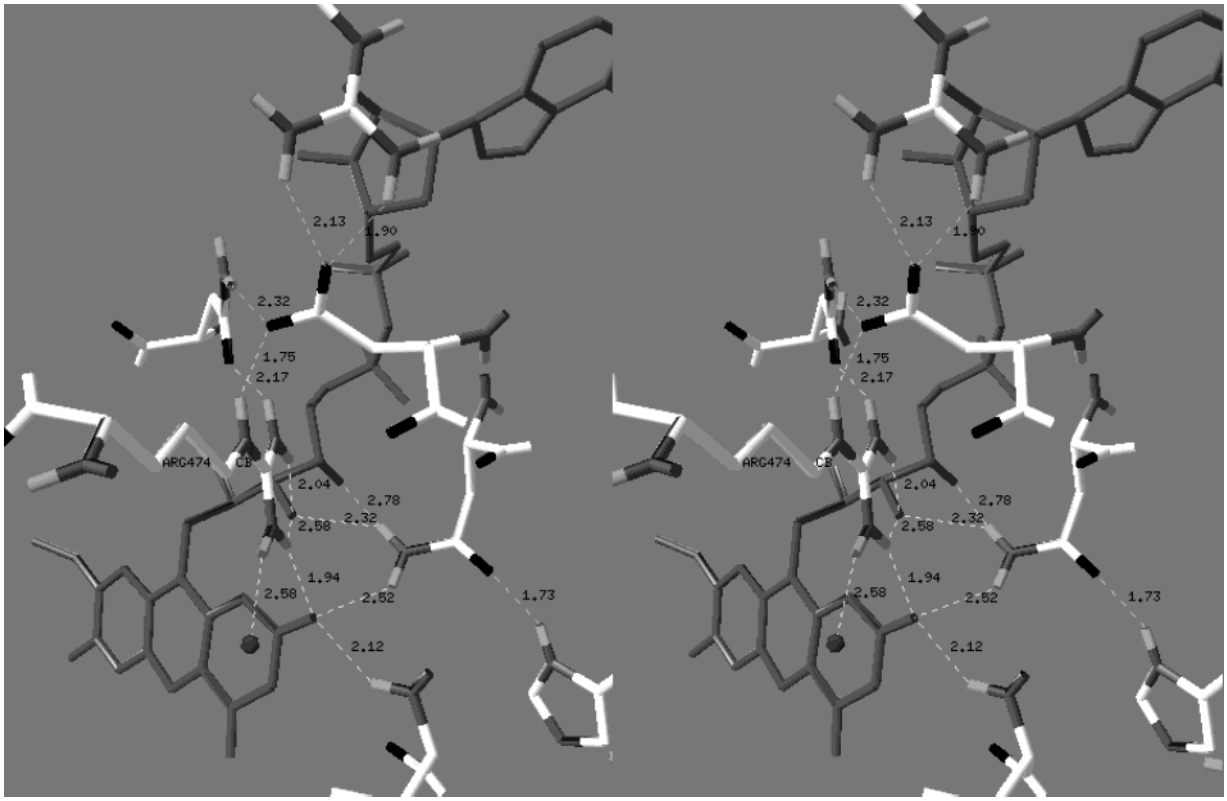

FIGURE 2: Stereoimage of the hydrogen-bonding network in the vicinity of Arg474 of PchF. Arg474, extending into the foreground, is labeled. Hydrogen bonds (thin dashed lines) and their distances in angstroms are displayed. Carbon, hydrogen, nitrogen, and oxygen atoms are white, gray, dark gray, and black, respectively. The small sphere at the bottom/middle of the image represents a water molecule.

linked to PchF[R474K]^{NC} to give PCMH[R474K]^{C}. The resulting flavocytochrome catalyzed the oxidation of phenolic substrates, albeit at a reduced rate when compared to PCMH. As described herein, PchF[R474K]^{C}, PchF[R474K]^{NC}, and PCMH[R474K]^{C} displayed some interesting changes in redox characteristics and other properties when compared to their wild-type counterparts.

EXPERIMENTAL PROCEDURES

Materials: Chemicals. FAD, bovine liver catalase, toluidine blue, gallocyanine, Nile blue, indigo trisulfonate, xanthine, xanthine oxidase (grade III from buttermilk), pepsin, phenazine ethosulfate (PES), and 1,3-bis[tris(hydroxymethyl)methylamino]propane (BisTrisPropane or BTP; Ultra grade) were from Sigma Chemical Co. Sodium dithionite was purchased from Fluka Chemical Corp., and 2,6-dichlorophenol indophenol (DCIP) was purchased from General Biochemical. 4-Bromophenol, 4-hydroxybenzyl alcohol, 4-hydroxybenzaldehyde (purified as described earlier, ref *10*), *p*-cresol (Gold Label grade), and 1-methylguanidine hydrochloride were purchased from Aldrich Chemical Co. Glucose oxidase was obtained from Miles Biomedical Research Products.

Methods: Site-Directed Mutagenesis of PchF. Synthetic oligonucleotides were purchased from Operon Technologies, Inc. Recombinant proteins were produced in *E. coli* BL21-(DE3) (Novagen, Inc.), and the first transformation step during the site-directed mutagenesis protocol utilized *E. coli* BMH71-18 *mut*S (Clontech Laboratories). All other molecular biology experiments utilized *E. coli* DH5αF′IQ (Gibco-BRL, Life Technologies, Inc) as the host.

The replacement of Arg474 in PchF with Lys or Ala was carried out by oligonucleotide-directed mutagenesis (*14*) by using the Transformer Site-Directed Mutagenesis kit (Clontech). The template was pUC19 containing a 627 bp *Asp*718/*Bam*H I DNA fragment from the 3′-end of the *pchF* coding sequence, derived from plasmid pKSII-PchF (*10*) and cloned into the same sites in pUC19. The mutagenesis was carried out by using Trans Oligo *Nde* I/*Nco* I

(5′-pGAG.TGC.ACC.ATG.GGC.GGT.GTG.AAA.T-3′) as the selection primer (provided with the Transformer kit) and either oR474K or oR474A

(5′-pGGC.TAT.GCG.GTG.TAT.AAG.GTG.AAC.ACG.CGT.TTC.CAG.GAT.CGC.G-3′ or

5′-pGGC.TAT.GCG.GTG.TAT.GCG.GTG.AAC.ACG.CGT.TTC.CAG.GAT.CGC.G-3′, respectively) as the mutagenic primer. The underlined bases differed from those of the target template. The mutagenesis protocol is described elsewhere (*15*). Two silent mutations within the codons for Thr477 and Arg478 were used to introduce a unique restriction site (A/CGCGT) for *Mlu* I as an aid to identify mutants. The *Asp*718/*Bam*H I inserts of selected mutants were sequenced in their entirety at the University of California, San Francisco Biomolecular Resource Center. The *Asp*718/*Bam*H I inserts of successful mutants were used to replace the native *Asp*718/*Bam*H I fragment in pET-PchF (*10*). After the transfer, the identities of the mutants, pET-PchF[R474K] and pET-PchF[R474A], were reconfirmed by sequencing across the mutated sites with T7 reverse primer. *E. coli* BL21(DE3) transformed with pET-PchF[R474K] or pET-PchF[R474A] was used for the production of the recombinant mutant PchF proteins.

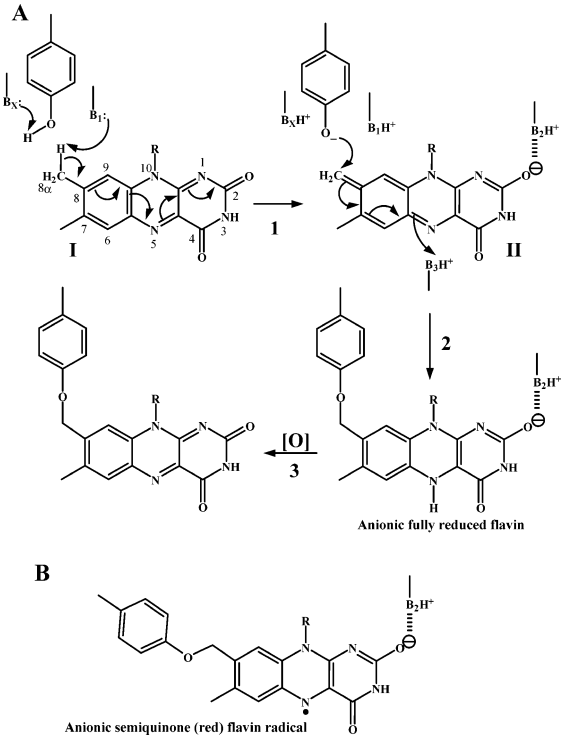

FIGURE 3: (A) Proposed mechanism for the covalent flavinylation of Tyr384 in PchF. The flavinylation process occurs only following the binding of PchC to $PchF^{NC}$ (*1*, *9*, *12*). B_X, B_1, B_2, and B_3 are bases of $PchF^{NC}$ in close proximity to the FAD. The base B_X (possibly Asp440; ref *6*) removes the phenolic proton from Tyr384 (Species **I**, with the positions of the isoalloxazine ring of flavin numbered), while base B_1 (again, possibly Asp440; ref *6*) removes a proton from the 8α carbon of the isoalloxazine ring of FAD (Step 1). This results in the formation of the requisite iminoquinone methide intermediate (Species **II**). An increase in the two-electron $E_{m,7}$ (i.e., the electrophilicity) of the flavin would make an 8α proton more acidic, thus facilitating the covalent flavinylation process. The anionic fully reduced form of the flavin is displayed also. (B) Structure of the anionic semiquinone (red) flavin radical. In both A and B, R represents the ribityl-diphospho-adenosine moiety of FAD.

Heterologous Production and Purification of PchF-[R474K], PchF[R474A], and PchC. E. coli strain BL21(DE3) containing plasmid pET-PchF[R474K] was grown aerobically in a 12-L fermentor. Cell harvesting, the production of periplasmic extracts with polymyxin B treatment, the addition of FAD to the extracts, and ion-exchange and hydroxyapatite chromatographies were performed as described previously (*10*). Purified PchF[R474K] was determined to be ~98% pure (SDS−PAGE) and to be free of FAD. Purified apo-PchF[R474K] was dialyzed for 6 h at 4 °C against a 25 mM BTP -HCl buffer at pH 7.5 and stored at −70 °C. Apo-PchF[R474A] was purified and stored in the same manner. $PchF^{C}$ was prepared as described previously (*10*).

In small-scale experiments for determining the relative rates of covalent binding of FAD to apo-PchF and to apo-PchF[R474K], PchC was isolated from purified *P. putida* produced PCMH by isoelectric focusing (IEF) (*7*, *9*, *16*, *17*). For other experiments, the source of PchC was the recombinant form isolated from *Pseudomonas aeruginosa* PAO1-LAC (*18*).

Mass Spectral Analyses. Mass spectral analyses of peptic fragments from $PchF[R474K]^{C}$ were carried out by the Protein Structure Core Laboratory at SUNY Downstate Medical School, Brooklyn, NY. FAD-containing peptides were converted to the FMN form, and the major FMN-containing peptide was isolated following the published procedures (*4*). The peptide was analyzed by electrospray ionization MS/MS. Tryptic fragments of apo PchF[R474K] were analyzed by LC-MS/MS and MALDI-TOF mass spectrometry.

Preparation of $PchF[R474K]^{C}$ and $PCMH[R474K]^{C}$. $PchF[R474K]^{C}$ was prepared by incubating 100−300 nmol of apo-PchF[R474K] with a 5-fold molar excess of PchC and a 20-fold molar excess of FAD in a 25 mM BTP-HCl buffer at pH 7.5, in 10−20 mL, for 1 h at 30 °C. The covalent flavinylation of PchF[R474K] was followed by monitoring the increase in absorbance at 552 nm because of the reduction of the heme in PchC (*9*, *10*). $PchF[R474K]^{C}$ was separated from PchC and a trace of nonflavinylated PchF[R474K] by IEF as described previously (*7*, *9*, *17*). $PCMH[R474K]^{C}$ was produced by incubating 5 μM $PchF[R474K]^{C}$ with 5 μM PchC in a 50 mM KH_2PO_4/KOH buffer at pH 7.3, for 30 min at 25 °C.

Characterization of $PchF[R474K]^{NC}$, $PchF[R474K]^{C}$, and $PCMH[R474K]^{C}$. UV−visible spectra were recorded with a Hewlett-Packard 8453 diode-array spectrophotometer, while single-wavelength kinetic traces were obtained with a Kontron Uvikon 943 split-beam spectrophotometer. The concentrations of the apo-PchF[R474K] solutions were determined by using $\epsilon_{280} = 81.4\ mM^{-1}\ cm^{-1}$ (*19*). Solutions of $PchF[R474K]^{C}$ were quantified by using $\epsilon_{450} = 11.8\ mM^{-1}\ cm^{-1}$, which was estimated from a solution of $PchF[R474K]^{C}$ in a 25 mM BTP-HCl buffer at pH 7.5, before and after denaturation with 2% SDS. The ϵ_{442} for FAD of the denatured protein was equal to that for free FAD in a 2% SDS solution ($\epsilon_{442} = 11.3\ mM^{-1}\ cm^{-1}$).

The affinity of apo-PchF[R474K] for FAD was measured by monitoring flavin-fluorescence quenching during the titration of a 5 μM FAD solution with increasing amounts of PchF[R474K] from 0 to 10 μM. The fluorescence was monitored with a Hitachi F-4010 Fluorescence spectrophotometer (excitation wavelength = 446 nm, excitation band-pass = 3 nm, emission wavelength = 520 nm, and emission band-pass = 10 nm).

The affinity of $PchF[R474K]^{C}$ for PchC was determined from the tryptophan-fluorescence quenching of PchF-$[R474K]^{C}$ by PchC (excitation wavelength = 280 nm, excitation band-pass = 3 nm, emission wavelength = 334 nm, and emission band-pass = 3 nm). The titration was carried out by successive additions of PchF[R474K] (0−2 μM) to a 1 μM solution of PchC. Both titrations were carried out in a 25 mM BTP-HCl buffer at pH 7.5 and 25 °C.

Anaerobic reductive titrations of PchF $[R474K]^{C}$ and $PCMH[R474K]^{C}$ were performed as before (*10*, *20*) in a 25 mM KH_2PO_4/KOH buffer at pH 7.25. *p*-Cresol ($\lambda_{max} = 276$ nm) and 4-hydroxybenzyl alcohol ($\lambda_{max} = 274$ nm) solutions were quantified by using $\epsilon(\lambda_{max}) = 1710\ M^{-1}\ cm^{-1}$.

p-Cresol and 4-hydroxybenzyl alcohol solutions were prepared in a buffer containing 10 mM glucose, 0.8 units of glucose oxidase, and 342 units of catalase to scavenge residual O_2 and partially deaerated with 7 vacuuming/flushing cycles with argon in an anaerobic vessel.

The two-electron redox midpoint potentials ($E_{m,7}$, NHE) of the FAD bound in $PchF[R474K]^{C}$ and of the FAD and

the heme bound in PCMH[R474K]^C were determined by using the method of Massey (*21*). The electrons resulting from the oxidation of xanthine by xanthine oxidase were transferred via the mediator, methyl viologen, to and between the redox protein of an unknown potential and a dye of known potential. Solutions of PchF[R474K]^C or PCMH-[R474K]^C (5−10 μM in a 50 mM KH_2PO_4/KOH buffer at pH 7.0) contained 200 μM xanthine, 2 μM methyl viologen, and sufficient dye for a maximal absorbance of 0.1−0.2. These solutions were made anaerobic by 20 cycles of vacuuming/flushing with argon in an anaerobic cuvette. Under anaerobiosis, xanthine oxidase (1−5 μg) was added via the sidearm of the cuvette and mixed with the solution to initiate the reaction. The values of $\log(P_{ox}/P_{red})$ (P = protein) were plotted against the values of $\log(Dye_{ox}/Dye_{red})$ to obtain the difference in redox potentials between the bound redox prosthetic groups and the dye (*21*).

To determine the values for the two one-electron redox midpoint potentials (E_1 and E_2, NHE) for PchF^C (*12*) and PchF[R474K]^C, these proteins were reduced with xanthine (300 μM) and xanthine oxidase (50 nM), in the presence of methyl viologen (20 μM) but in the absence of a reference dye, in a 50 mM KH_2PO_4/KOH buffer at pH 7.0 and 25 °C. Under these conditions, the complete two-electron reduction of PchF[R474K]^C and PchF^C (*12*) proceeded with the intermediate formation of the anionic flavin semiquinone radical. The procedure for determining the one-electron potential values from the resulting spectral data can be found in ref *12* and is described in more detail in the Supporting Information.

The typical application of the xanthine/xanthine oxidase method for determining the $E_{m,7}$ (NHE) for PchF[R474K]^{NC} is complicated by the fact that FAD binds relatively weakly ($K_D \approx 2$ μM). Additionally, there are no significant changes in the spectrum of FAD upon binding, so factor analysis could not be applied. A modified xanthine/xanthine oxidase method that was used for determining the $E_{m,7}$ value is presented in the Supporting Information. Indigo trisulfonate ($E_{m,7} = -81$ mV) and Nile blue ($E_{m,7} = -119$ mV) were used as reference dyes. The concentrations of both FAD and the protein were 21 μM in a BTP-HCl buffer (25mM) at pH 7.0 ($T = 25$ °C).

The factor analyses of UV−visible spectral titrations were accomplished using SPECFIT (Spectrum Software Associates, Chapel Hill, NC).

Steady-State and Stopped-Flow Kinetic Studies. Steady-state kinetic assays, which monitored the reduction of 2,6-dichlorophenol indophenol (DCIP) by the enzyme-reduced electron-accepting substrate, phenazine ethosulfate (PES), were carried out at 25 °C as described previously (*3*, *22*).

Stopped-flow studies were carried out in a 25 mM KH_2PO_4/KOH buffer at pH 7.2 and 25 °C using an OLIS RSM-16 rapid-scanning instrument (On-Line Instruments Systems, Inc., Bogart, GA). The substrate reduction of PchC in the flavocytochrome was monitored. Data were analyzed by using the OLIS GLOBAL analysis (3D), kinetic analysis (2D), and spectral reconstruction software.

RESULTS

Binding of FAD to PchF[R474K] and PchF[R474A]. Apo-PchF[R474K] bound FAD noncovalently ($K_D \approx 2$ μM at pH 7.5 and 25 °C) more weakly than did wild-type apo-PchF (the K_D value was too low to measure by the fluorescence-quenching method). In comparison to apo-PchF, apo-PchF[R474K] bound FAD covalently in the presence of PchC at a reduced rate at 25 °C as monitored by the reduction of the PchC at 552 nm (*9*, *10*). In the presence of 15 μM FAD and 15 μM PchC, the FAD first bound noncovalently and then covalently to apo-PchF[R474K] (7 μM) with an observed rate constant of 0.03 min^{-1} in a 50 mM KH_2PO_4/KOH buffer at pH 7.0. This rate constant is 0.62 ± 0.06 min^{-1} for the formation of wild-type PCMH from apo-PchF, FAD, and PchC.

Under similar conditions, efforts to bind FAD covalently to apo-PchF[R474A] in the presence of PchC were unsuccessful, although the addition of 0.1 M 1-methylguanidinium provided a slow rate of product formation. It was thought that this compound would diffuse into the void left by the missing guanidino group of Arg474, now occupied partially by the methyl group of Ala. Once properly positioned, the protein-bound 1-methylguanidinium might catalyze the covalent flavinylation of Tyr384. The extremely slow reduction of PchC was not observed when 1-methylguanidinium, FAD, or PchF[R474A] were excluded from the reaction mixture. However, it was estimated that it would take weeks for a complete covalent flavinylation of all of the PchF[R474A] to occur under these conditions.

The UV−visible spectrum of PchF[R474K]^C had an A_{280}/A_{447} ratio (9.0:1) that was similar to that for PchF^C (9.1:1), indicating a stoichiometric incorporation of FAD into PchF-[R474K]^C. However, the absorbance maxima for the attached flavin were shifted to longer wavelengths for PchF[R474K]^C (369 and 447 nm) when compared with those of wild-type PchF^C (363 and 442 nm) (spectral data not shown).

Mass spectral analysis of PchF[R474K]^C provided a M_r of 58 563 ± 6 mass unit, in exact agreement with the predicted mass. An electrospray-ionization MS/MS analysis of the major peptic FMN-containing peptide, derived from PchF[R474K]^C, provided parent-ion masses of 1091 (M + H) and 546 (M + 2H). The masses of various fragments indicated that the peptide had the composition YNWR, with FMN attached to Y. This sequence is unique in PchF-[R474K]^C. MALDI-TOF mass spectral analysis of a tryptic digestion of PchF[R474K]^C yielded a mass expected for a flavopeptide from PchF[R474K]^C with the composition AQLMSGVPNLQEFGLYNWR, where Y is Tyr384, the site of FAD attachment. These results established unambiguously that FAD is covalently linked to Tyr384, as it is for wild-type PchF^C. Mass spectral analysis confirmed also that Arg474 was replaced by Lys; the sequence of a tryptic peptide was found to be EGYAVYK474.

Binding of PchF[R474K]^C to PchC. A K_D value for the interaction of PchF[R474K]^C with PchC was determined to be 130 ± 60 nM, which is greater than that determined for the binding of PchC to PchF^C under similar conditions ($K_D = 7.4 \pm 0.4$ nM) (*18*) but considerably smaller than the value determined for the PchF[Y384F]^{NC}·PchC complex ($K_D = 7.4 \pm 0.7$ μM), where FAD is bound noncovalently (*12*).

Titrations of PchF[R474K]^{NC} and PchF[R474K]^C. The redox and spectral properties of PchF[R474K]^{NC} and PchF-[R474K]^C were studied by conducting anaerobic titrations with dithionite, *p*-cresol, and 4-ethylphenol, and aerobic titrations with 4-hydroxybenzaldehyde and 4-bromophenol. More complete descriptions of most of these titrations can

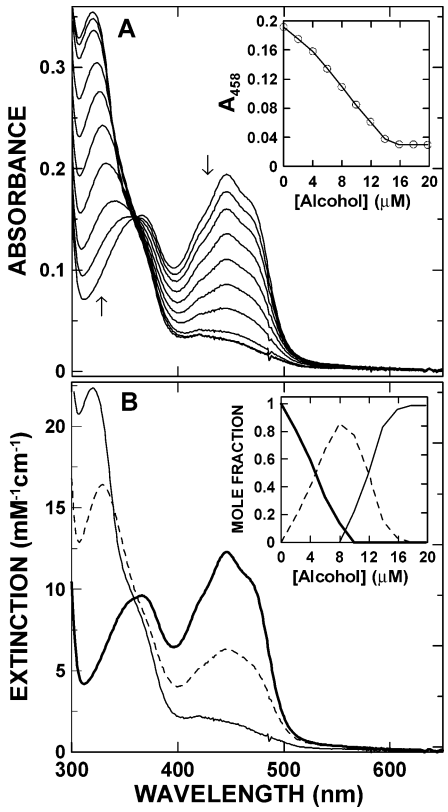

FIGURE 4: Spectra for the anaerobic titration of PchF[R474K]^{C} with 4-hydroxybenzyl alcohol. A 1.5-mL solution of 16 μM PchF-[R474K]^{C} in a 25 mM KH_2PO_4/KOH buffer at pH 7.25 was titrated with a solution of 4-hydroxybenzyl alcohol, at 25 °C. (A) Recorded spectra are shown for 0, 2.0, 4.0, 7.0, 8.0, 9.9, 11.9, 13.9, 15.8, 17.8, and 19.7 μM alcohol. The arrows indicate the changes that occurred as more alcohol was added. The inset shows a plot of the absorbance at 447 nm versus the alcohol concentration. (B) This frame displays the spectra derived from the factor analysis of the spectral data shown in A. In the main and inset frames, the bold line is that recorded for untreated PchF[R474K], the dashed line for the intermediate form, and the thin solid line for fully (2-electron) reduced PchF[R474K] and free 4-hydroxybenzaldehyde.

be found in the Supporting Information for this paper. Here, we present the salient features of the experiments.

The stoichiometric dithionite titration of PchF[R474K]^{NC} proceeded without the intermediate formation of a flavin radical, whereas an anionic "red" flavin radical did appear during the stoichiometric dithionite titration of PchF-[R474K]^{C} (Figure 1S in the Supporting Information). When titrated with *p*-cresol, PchF[R474K]^{NC} was not reduced, but a charge-transfer complex (CTC) formed between the substrate and bound FAD. When PchF[R474K]^{C} was titrated anaerobically with *p*-cresol, apparent end-point spectra were reached within 15 min after the addition of each aliquot of the titrant. However, the addition of 1 equiv of *p*-cresol resulted in an approximately 50% reduction of the flavin.

The anaerobic spectrophotometric titration of PchF[R474K]^{C} with 4-hydroxybenzyl alcohol resulted in a rapid, stoichiometric and complete reduction of the flavin (Figure 4) with concomitant formation of 1 equiv of 4-hydroxybenzaldehyde, as monitored by the absorbance increase at 323 nm. This titration proceeded in a manner similar to that observed for the anaerobic titration of PchF^{C} with this substrate (*10*). In the course of the titration, two isosbestic points were revealed (the 340−360-nm region) (Figure 4). This indicates that three independent components (factors) were involved in the transition from fully oxidized to fully reduced FAD. A factor analysis of the data (Figure 4B) shows that, after the addition of 0.5 electron equiv, 87% (inset of Figure 4B) of the total protein is represented by a species that has an intermediate spectrum with $\lambda_{max} = 330$ nm. This converted to the final spectrum with $\lambda_{max} = 320$ nm on the addition of the second 0.5 electron equiv with a concomitant shift of the isosbestic point from 360 to 338 nm. These transitions are not unique to PchF[R474K]^{C}, because they were also seen during the titrations of either PchF^{C} or PchF[Y384F]^{NC} with 4-hydroxybenzyl alcohol (*10*, *12*). An interpretation of these findings is offered in the Discussion.

Aerobic titrations with 4-hydroxybenzaldehyde yielded K_D values of 7 (estimated) and 3.4 ± 0.3 μM for PchF[R474K]^{NC} and PchF[R474K]^{C} (Figure 2S in the Supporting Information), respectively. This value for PchF^{C} was 0.81 μM (*10*). In all cases, the aldehyde was bound in its anionic quinonoid form (*10*) as a CTC with FAD.

Similar aerobic titrations of PchF[R474K]^{NC} and PchF-[R474K]^{C} with 4-bromophenol, a substrate mimic that, like 4-hydroxybenzaldehyde, cannot reduce the enzyme, yielded CT complexes with K_D values of 51 and 16 ± 4 μM, respectively, the latter value being identical to that determined for the PchF^{C}·4-bromophenol complex (*10*). For PchF-[R474K]^{NC}, the $\lambda_{max} \approx 550$ nm is red-shifted considerably from the λ_{CT} (629 nm) found for the PchF[R474K]^{C}·4-bromophenol complex. This corresponds to a change of 300 mV, which reflects a shift in the redox potential of the acceptor, FAD [+30 mV − (−106 mV) = 136 mV] and a contribution from a change for the donor, 4-bromophenol (300 mV − 136 mV = 164 mV) (vide infra and Table 1). Thus, both shifts contribute to the increased energy of the CT band for PchF[R474K]^{NC} relative to that for PchF-[R474K]^{C}.

Titrations of PCMH[R474K]^{C}. The CTC between 4-bromophenol and the covalently bound FAD of PCMH[R474K]^{C} was studied. PchF[R474K]^{C} was saturated with a 20-fold excess of 4-bromophenol and then titrated with PchC. Factor analysis revealed three independent spectra, the PchF[R47-4K]^{C}·4-bromophenol complex, free PchC, and the PCMH-[R474K]^{C}·4-bromophenol complex. After the contribution from PchC in the last spectrum was subtracted, the spectrum of a CTC was obtained (Figure 5). The new CT-peak is red-shifted compared to the CT-peak for PchF[R474K]^{C}·4-bromophenol; however, the extinction coefficient for the peaks for the two CT complexes are about the same. This indicates that PchC does not change the overlap of the π orbitals for 4-bromophenol and FAD, but rather it changes the difference between the ionization potential (I^D) of 4-bromophenol and/or the electron affinity (E^A) of the flavin, which defines the wavelength of maximum absorbance; $h\nu_m = I^D - E^A$, where h is Planck's constant and ν_m is the frequency of the maximum absorbance of the CT peak (*23*).

PCMH[R474K]^{C}, derived by mixing equimolar amounts of PchF[R474K]^{C} and PchC, was titrated anaerobically with *p*-cresol. The addition of approximately 0.25 equiv of the substrate resulted in PCMH[R474K]^{C} containing fully reduced heme and fully oxidized FAD (data not shown). Because PchC cannot be reduced directly by *p*-cresol, the flavin in the active site of PCMH[R474K]^{C} was reduced transiently by the substrate, and the two electrons in fully

Table 1: Redox and Spectral Properties for Various Proteins

protein[a]	k_{cat} (s^{-1})[b]	$E_{m,7}$ (mV)[c]	λ_{CT} (nm)	E_{CT} (mV)	ΔE_{CT} (mV)[d]	α[e]
PCMH	121	92.5	833	1490	0	NA [f]
E_1[g]		136				
E_2		49				
$PchF^{C}$[h]	2.4[i], 4.4[j]	62	680	1825	335	0.29, 0.25
E_1[j]		129				
E_2		−5				
PCMH[R474K]^{C}	2.4	82[k], 74[l], 78[m]	693	1791	301	0.33
E_1		132[l], 124[m]				
E_2		16[l], 32[m]				
PchF[R474K]^{C}	0.26	30	629	1973	483	0.32
E_1		128				
E_2		−68				
$PchF^{NC}$ [h]	0.08	−16	620	2002	512	0.36
E_1		26				
E_2		−55				
PchF[R474K]^{NC}	0.01	−106	546	2273	783	0.32
PCMH {heme}[h]	NA	234	NA	NA	NA	NA
PCMH[R474K] {heme}	NA	228	NA	NA	NA	NA
PchF[R474K]^{C}·aldehyde[n]	NA	9	NA	NA	NA	NA

[a] The proteins are listed in order of decreasing k_{cat} values. [b] The k_{cat} values were determined under identical conditions, using *p*-cresol as the substrate. [c] The redox potentials are for FAD bound to the protein except where noted. [d] $\Delta E_{CT} = E_{CT,protein} - E_{CT,PCMH}$. The energy values were calculated from the λ_{CT} values; $E_{CT} = hc/\lambda_{CT}$, where h (Planck's constant) = 4.1227×10^{-15} eV s and c (the speed of light) = 2.9979×10^{17} nm/s. [e] $\alpha = -25\ mV \times \ln(k_{cat,protein}/k_{cat,PCMH})/\Delta E_{CT}$. [f] Not applicable. [g] E_1 and E_2 are the values for the two one-electron potentials of the bound flavin. [h] The values for the redox potentials are from ref 12. [i] See ref 3. [j] See ref 7. [k] Determined by using the xanthine/xanthine oxidase procedure. [l] Determined from the *p*-cresol titration of this protein. [m] Determined from the dithionite titration of this protein. [n] The redox potential was measure for the FAD bound to the PchF[R474K]^{C}·4-hydroxybenzaldehyde complex.

reduced FAD were transferred rapidly intra- and intermolecularly to PchC. The further addition of about 0.5 equiv of the substrate resulted in the full reduction of the FAD in PCMH[R474K]^{C}.

PCMH[R474K]^{C} was titrated also using dithionite as the reductant, and the titration proceeded in a similar manner (data not shown). For comparison, we have also repeated a dithionite titration of wild-type PCMH (*3*, *22*), under the same conditions. Again, the heme reduction was nearly complete prior to the appearance of the FAD radical, which, as with PCMH[R474K]^{C}, each step required 1-electron equiv/mol of enzyme.

Measurement of the Redox Potentials for PchF[R474K]^{C} and PchF[R474K]^{NC}. The two-electron midpoint potentials ($E_{m,7}$, NHE) for the flavins in PchF[R474K]^{C} and PchF[R474K]^{NC} were determined by using the xanthine/xanthine oxidase system (or a modification thereof) and different reference redox dyes (*21*). The two-electron $E_{m,7}$ value for FAD in PchF[R474K]^{C} was found to be 30 or 31 mV when using either gallocyanine or toluidine blue, respectively, as the redox dye. These values are lower than the value of 62.5 mV determined for $PchF^{C}$ (*12*).

The factor analysis of the spectra obtained from the reduction of $PchF^{C}$ and PchF[R474K]^{C} by the xanthine/xanthine oxidase/methyl viologen electron-generating system provided values of 0.87 (*12*) and 0.94 for the expression $[\text{flavin radical}]_{max}/[\text{flavin}]_{total}$, for $PchF^{C}$ and PchF[R474K]^{C}, respectively. Using these data and an established procedure (*12*, *24*), the difference between the redox potentials for the first and second 1-electron processes, $\Delta E = E_1 - E_2$, were calculated. The ΔE values are 133 and 176 mV for $PchF^{C}$ and PchF[R474K]^{C}, respectively. Because $(E_1 + E_2)/2 = E_{m,7}$, then $E_1 = E_{m,7} + \Delta E/2$ and $E_2 = E_{m,7} - \Delta E/2$. For $PchF^{C}$, $E_{m,7} = 62.5$ mV, and therefore $E_1 = 129$ mV and $E_2 = -5$ mV (*12*), and for PchF[R474K]^{C}, $E_{m,7} = 30$ mV, and therefore $E_1 = 128$ mV and $E_2 = -68$ mV.

Because 4-hydroxybenzaldehyde is bound tightly, the redox potential for the flavin in the complex PchF[R474K]^{C}·aldehyde may be determined and was found to be 9 mV (using gallocyanine), 21 mV lower than that for bound FAD when the aldehyde is absent.

Because of the weak binding of FAD to PchF[R474K] ($K_D^{ox} \approx 2\ \mu M$) and the lack of detectable absorbance differences for bound and free FAD, the measurement method and data analysis for determining the $E_{m,7}$ value for PchF[R474K]^{C} required modification, as mentioned in the Experimental Procedures. A complete description of the analysis is provided in the Supporting Information. It was determined that the two-electron $E_{m,7}$ for PchF[R474K]^{NC} was −101 or −106 mV when Nile blue or indigo trisulfonate, respectively, was used as the reference redox dye. For comparison, the two-electron $E_{m,7}$ for $PchF^{NC}$ is −16 mV.

Measurement of the Redox Potentials for PCMH[R474K]^{C}. For the FAD of PCMH[R474K]^{C}, the two-electron $E_{m,7}$ value was found to be 82 or 81 mV when using toluylene blue or thionin, respectively, as the reference dye. These values are similar to that determined for PCMH (92.5 mV). The $E_{m,7}$ value for the heme in PCMH[R474K]^{C} was found to be 228 mV using DCIP as the reference dye, a value similar to that of 234 mV for the heme in PCMH (*12*). Hence, the reduced catalytic activity of PCMH[R474K]^{C} appears to be due to factors other than different redox potentials of the prosthetic groups for the two forms of PCMH.

For the reductive titrations of PCMH and PCMH[R474K]^{C}, we invoked the same procedure that was used previously (*12*) to determine the 1-electron $E_{m,7}$ values of the FAD bound to PCMH[Y384F]^{NC}. For this method, the $E_{m,7}$ values of the heme were used as reference points for the determinations, and it was assumed that there was a rapid electron equilibration among the various redox species. The values of E_1, E_2, and the 2-electron potential $E_{m,7}$ ($=[E_1 + E_2]/2$) measured by this procedure are listed in Table 1.

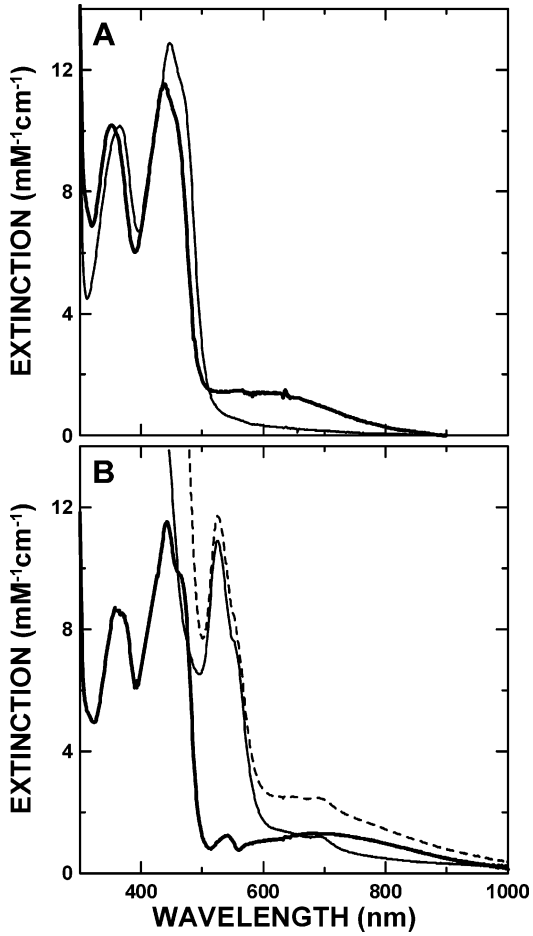

FIGURE 5: Spectra for the CT complexes of 4-bromophenol with PchF[R474K]^{C} and PCMH[R474K]^{C}. (A) Spectra of the PchF-[R474K]^{C}·4-bromophenol complex (thick solid line) and the free flavoprotein (thin line). (B) Spectra of PCMH[R474K] (thin solid line), the PCMH[R474K]·4-bromophenol complex (dashed line), and the difference spectrum (thick solid line). The latter reveals a red-shift of the λ_{max} of CTC compared to that displayed in A.

Steady-State and Stopped-Flow Kinetic Studies. Steady-state kinetic assays for PchF[R474K]^{NC} were carried out with *p*-cresol as the reducing substrate and PES as the electron accepting substrate. Because of the slow reaction, a high concentration of the protein was required. For each assay, the concentration of apo-PchF[R474K] was 3.25 μM and that of [FAD] was 52 μM; on the basis of a $K_D \approx 2$ μM, the concentration of PchF[R474K]^{NC} was estimated to be 3.2 μM. From these studies, a $k_{cat} = 0.0051$ s^{-1} was determined for PchF[R474K]^{NC}, which is considerably slower that that found for PchF[R474K]^{C} or PchF^{C} (vide infra).

The steady-state kinetic parameters for PCMH[R474K]^{C} were determined also using *p*-cresol and PES as the substrates. The K_M value for *p*-cresol was determined to be 25 μM, which is similar to that observed for PCMH (*18*, *22*). The value of k_{cat}, however, was found to be 2 s^{-1}, which is about 40 times lower than that determined for PCMH (*18*, *22*). The value of k_{cat} for PchF[R474K]^{C} was 0.26 s^{-1}, whereas this value was 4 s^{-1} for PchF^{C}. The $K_{M,p-cresol}$ values are 27 μM for PchF[R474K]^{C} and 25 μM for PchF^{C}.

The reactions of *p*-cresol and *p*-cresol-α,α,α-d_3 (4-[$^2H_3$]-methylphenol) with PCMH[R474K]^{C} were followed also by stopped-flow spectroscopy (*12*). The rate constants for the isotopically sensitive step are independent of the substrate concentration and equal to 2.41 and 0.32 s^{-1} for *p*-cresol and *p*-cresol-α,α,α-d_3, respectively, which yield an intrinsic primary deuterium kinetic isotope effect (KIE) of 7.5, the same within the experimental error to those found for PCMH and PCMH[Y384F]^{NC} (*12*, *25*). The steady-state kinetic primary deuterium KIE [$^D(k_{cat}/K_M)$] was found to be 6.4 for PCMH[R474K]^{C}, which is similar to that determined for PCMH. The similarities of these values suggest that each enzyme variant oxidizes the substrate via identical mechanisms. The stopped-flow rate constants were determined by analyzing the spectral changes for heme reduction. The findings that these constants provide the expected value for the intrinsic primary deuterium KIE indicate that the two-electron substrate reduction of FAD must be significantly slower than the electron transfer from fully reduced FAD to heme.

DISCUSSION

Correlation between the Values of k_{cat}, Redox Potentials, and Spectral Properties of CT Complexes with 4-Bromophenol. On completion of the steady-state kinetic studies with PchF[R474K]^{C}, PchF[R474K]^{NC}, and PCMH[R474K]^{C}, we compiled all of the data for these enzymes along with the same data for their corresponding wild-type forms (Table 1). It was immediately apparent that the k_{cat} values for *p*-cresol oxidation decreased in a uniform fashion for the various forms of the PchC-free and PchC-complexed PchF species as the wavelengths of maximal absorbance, λ_m, for the 4-bromphenol CT bands decreased (Table 1). The $E_{m,7}$ (2-electron potential) values decreased also, but the correlation was less impressive; for example, because both PCMH and PCMH[R474K] have nearly identical $E_{m,7}$ values, one might predict that they would have similar k_{cat} values, but that is not the case.

The frequency of the maximal absorbance for a CT band, ν_m ($=c/\lambda_m$, where c is the speed of light), can be defined by $h\nu_m = I^D - E^A$ (*23*), where h is Planck's constant, I^D is the ionization potential of the donor (4-bromophenolate), and E^A is the electron affinity of the acceptor (protein-bond FAD). On the other hand, the rate of electron transfer from protein-bound *p*-cresolate to FAD may be expressed as exp-[$\alpha(E^A - I^D)/RT$], where $0 < \alpha < 1$ is the symmetry factor or transfer coefficient (*26*) and I^D is the ionization (redox) potential for *p*-cresol. Hence, the driving force of the redox reaction is represented by ($E^A - I^D$). Formally, $\alpha = d(\Delta G^{\ddagger})/d(\Delta G°) = d[\ln(k)]/d[\ln(K)]$, where $\Delta G^{\ddagger}$ is the change in the free energies between the reactants and the transition state ($=\Delta E$, the activation energy) and $\Delta G°$ is the change in the free energies between the reactants and products (*26*, *27*). This parameter is equivalent to the α coefficient in the Brønsted equation that relates a reaction rate constant, k, to the equilibrium constant, i.e., $k = AK^{\alpha}$ (*26*). It is believed to be a measure of the extent of the reaction from the reactant state to the transition state ($\alpha = 0$ for the reactant state, $\alpha = 1$ for the product state, and $\alpha = 0.5$ for a symmetrical transition state).

Although the electronic properties of *p*-cresol and 4-bromophenol are very different, they have similar structures because the methyl and bromo groups occupy approximately equal volumes. Presumably, with the same π-electron ring systems and orientation of the rings, both bind to PchF and

PCMH in a similar fashion as the phenolate forms (see Figure 1). For our purpose, it is assumed that the protein environment effects similar changes in the electronic properties of the FAD·4-bromophenolate and FAD·*p*-cresolate complexes by going from one form of PchF or PCMH to another. In other words, $\Delta(I^D - E^A)_{4-\text{bromophenol}} \approx \Delta(I^D - E^A)_{p-\text{cresol}}$. This assumption is corroborated by the work of Abramovitz and Massey (*28*) with old yellow enzyme (OYE) reconstituted with different FMN analogues. When the ν_{CT} values for a series of phenols bound to either the 7-bromo-FMN or 5-deaza-FMN forms of OYE were plotted against the ν_{CT} values for this series of phenols complexed with the native enzyme, the two linear plots were approximately parallel (*28*). Therefore, $\Delta(I^D - E^A)_{\text{phenol}-A} \approx \Delta(I^D - E^A)_{\text{phenol}-B}$ for OYE.

Because $h\nu_m = I^D - E^A$, differences in $(I^D - E^A)$ for the 4-bromophenol complexes of various forms of PchF and PCMH result in shifts of the maximum wavelength, λ_m (i.e., ν_m), of the CT bands. However, because $k = \exp[\alpha(E^A - I^D)\, F/RT] = \exp[\alpha(E^A - I^D)/kT]$, changes in $(I^D - E^A)$ lead to a reaction-rate change for the *p*-cresol complexes (see Table 1); for the equation, F is the Faraday constant, R is the gas constant, and k is the Boltzmann constant. Invoking the assumption that $\Delta(I^D - E^A)_{4-\text{bromophenol}} \approx \Delta(I^D - E^A)_{p-\text{cresol}}$, it is concluded that there is a linear relationship between ν_m and $\ln(k)$. This analysis indicates that a study of the spectral properties of the 4-bromophenol CT complexes with various forms of PchF and PCMH would allow us to construct a scale from which the reaction rates of *p*-cresol oxidation may be computed. It is important to note that correlations with either I^D or E^A separately are misleading, because both values are affected by the protein environment and by the interaction of the substrate with the flavin cofactor.

This approach is applied here to the oxidation of *p*-cresol by PchF[R474K]^C and PCMH[R474K]. From the kinetic studies, $k_{\text{PCMH[R474K]}}/k_{\text{PchF[R474K]}} = 2.4\ s^{-1}/0.256\ s^{-1} = 9.4$, while the λ_{max} of the 4-bromophenol CT peak shifts from 629 to 693 nm when PchC binds to PchF[R474K]^C, which translates into a potential change of 182 mV. It is assumed that $\Delta(I^D - E^A)_{4-\text{bromophenol}} = -182\ \text{mV} \approx \Delta(I^D - E^A)$ for the interactions of *p*-cresol with PchF[R474K]^C and PCMH-[R474K]^C. Using the existing data, we can estimate the values of ΔI^D and ΔE^A. ΔE^A is assumed to be equal to $\Delta E_{m,7}$ for FAD (*23*) in PchF[R474K]^C before and after this protein binds to PchC. Hence, $\Delta E^A \approx 82\ \text{mV} - 30\ \text{mV} = 52\ \text{mV}$ for the two-electron process; this calculation assumes that the value of $E_{m,7}$ for FAD in the flavocytochrome when the heme is oxidized is the same as that measured when the heme was reduced (Table 1). The ionization (redox) potential of the substrate is decreased by $\Delta I^D = -182\ \text{mV} + 52\ \text{mV} = -130\ \text{mV}$ for PchF[R474K]^C relative to the flavocytochrome. This indicates that *p*-cresol is a poorer reductant for PchF-[R474K]^C than it is for PCMH[R474K]^C. We conclude that the difference in the redox potentials for both the substrate and the cofactor contributes significantly to catalysis.

From the equation $k_{\text{PCMH[R474K]}}/k_{\text{PchF[R474K]}}{}^C = \exp[\alpha\Delta(E^A - I^D)/kT]$, we find that $\alpha = (25\ \text{mV}/182\ \text{mV})\ln(9.4) = 0.31$. This value, which is somewhat less than 0.5 for a symmetrical transition state, implies an "early" or "reagent-like" transition state. Note that the Marcus equation is $k_{ET} = \exp[-(\lambda + \Delta E)^2/4\lambda kT] = \exp(-\lambda/4kT - \Delta E/2kT - \Delta E^2/4\lambda kT)$. If we assume that the reorganization energy, $\lambda \gg \Delta E$, then $k_{ET} \approx \exp(-\Delta E/2kT) = \exp(\alpha[E^A - I^D]/kT)$, where $\Delta E = I^D - E^A$, and $\alpha = {}^1/_2$.

This approach may be also applied to the various forms of PchF[R474K] and to wild-type PchF (*12*), by using the data for intact wild-type PCMH as the reference. The results of this analysis are compiled in Table 1. The existence of the predicted correlation between the λ_{max} for the 4-bromophenol CT complexes and k_{cat} for six different protein species is evident from the inspection of the data (Table 1). The average value of α from the table is 0.31.

O*ther Aspects of Catalysis*. The ability of *p*-cresol to reduce different forms of PchF correlates roughly with the $E_{m,7}$ of the bound FAD. For example, *p*-cresol forms a CTC with PchF^{NC} ($E_{m,7} = -16$ mV) but does not reduce it. However, it reduces PchF[Y384F]^{NC} ($E_{m,7} = 2$ mV) very slowly, if at all, and, apparently, without CTC formation. This substrate reduces partially PchF[R474K]^C ($E_{m,7} = 30$ mV) but reduces rapidly and completely PchF^C ($E_{m,7} = 62$ mV). For the latter two cases, absorbances attributable to the CT complexes were not observed during stopped-flow kinetic studies. This implies that the *p*-cresol·FAD CTC formation and the ability of this substrate to reduce flavin are mutually exclusive. Consequently, CTC formation is not a prerequisite for catalysis but rather reflects the inability of *p*-cresol to react (*29*). From these observations, it is concluded that the redox potential of enzyme-bound *p*-cresol is similar in value to the potential of FAD in PchF[Y384F]^{NC}, i.e., 2 mV. For this flavoprotein, even if a CT band forms, it would be shifted to a far-red wavelength and would not be easily observable.

PchF[R474K]^C and PchF[R474K]^{NC}, like PchF^C and PchF^{NC}, bind substrate analogues such as 4-hydroxybenzaldehyde and 4-bromophenol, as their anionic phenolate forms (*10*). As with PchF^C and PchF^{NC} (*10*), these analogues formed CT complexes with the FAD bound to the two variants of PchF[R474K]. However, the latter affinities for 4-hydroxybenzaldehyde are less than those of PchF^C and PchF^{NC}, perhaps because of a change in the shape of the hydrophobic portion of the substrate-binding cavity of the flavoprotein (see Figure 1). The aliphatic portion of Arg474 is an important component of this region of the substrate-binding pocket of PCMH (*6*); it "pushes" the aromatic rings of Tyr95 and Tyr473 into position to hydrogen bond with the phenolic oxygen of *p*-cresol (Figure 1).

The redox potential of PchF[R474K]^C was decreased by 21 mV when 4-hydroxybenzaldehyde was bound. The equation $\exp[2 \times 21\ \text{mV}/25\ \text{mV}]$ indicates that the dissociation constant is 5.4 times larger for the reduced PchF[R474K]^C·aldehyde complex than for this complex in the oxidized form. Because the $K_D = 3.4\ \mu$M for the oxidized complex, then a $K_D = 18.4\ \mu$M may be calculated for the reduced complex. This conclusion facilitates the interpretation of the spectral data for the anaerobic reductive titration of PchF[R474K]^C by 4-hydroxybenzyl alcohol (Figure 4). Upon flavin reduction, the alcohol is converted to the aldehyde. We speculate that, after it dissociates from reduced PchF[R474K]^C, the aldehyde rebinds preferentially to oxidized PchF[R474K]^C. This prevents alcohol binding and subsequent FAD reduction. This process continues until approximately half of the PchF[R474K]^C is oxidized and has aldehyde bound, while the other half is reduced and relatively aldehyde-free. Reduction of the remaining oxidized flavopro-

tein by further additions of the alcohol is slow because it cannot bind until the tightly bound aldehyde dissociates. The final spectrum for the alcohol titration results from the combined absorbances of equimolar amounts of fully reduced PchF[R474K]^{C} and mostly enzyme-free 4-hydroxybenzaldehyde. This effect is more pronounced with PchF^{C} because its redox potential decreases by 60 mV upon complexing with the aldehyde (unpublished findings).

The k_{cat} value for *p*-cresol oxidation by PCMH[R474K]^{C} is 50-fold lower than that for PCMH. One might speculate that the lowered activity is a result of the altered two-electron midpoint potential for the FAD in PchF[R474K]^{C}, which is about 40 mV lower than that for the FAD in PchF^{C}. However, for PCMH, the two-electron $E_{m,7}$ for the FAD (92.5 mV) is similar to that for PCMH[R474K] (82 mV), which indicates that the oxidizing power of FAD in both forms of PCMH is comparable. In fact, stopped-flow kinetic studies, with *p*-cresol or *p*-cresol-α,α,α-d_3, indicated that heme reduction was slower for PCMH[R474K]^{C} than for PCMH. However, this is not due to a lower rate of electron transfer from reduced FAD to oxidized heme because the rate constants for this process provided the apparent intrinsic primary deuterium KIE of 7 for both forms of PCMH. Only when ET from reduced FAD to heme is considerably faster than the prior reduction of FAD by the substrate will the apparent rate constants for heme reduction provide the expected intrinsic primary deuterium KIE, as observed.

Covalent Flavinylation. The PchF[R474K] mutant was produced originally for the express purpose of testing the notion that Arg474 is essential for covalent FAD binding for PchF^{NC} when it is exposed to PchC. It is believed that a positive charge near the *C2* oxygen of the flavin ring is essential for its covalent attachment in various flavoenzymes whether it is tethered (Figure 3A) at the 8 methyl or the 6 position of the isoalloxazine ring (*11*). This positive charge is provided either by the side group of a lysyl or arginyl residue and/or the positive end of a helical dipole. This localized electrostatic field stabilizes the anionic semiquinone ("red") flavin radical (Figure 3B) that is observed for all covalent flavoproteins (*30*) and is believed to be important also for catalysis by stabilizing the anionic form of the fully reduced flavin (Figure 3A).

For PCMH, Arg474 provides the requisite positive charge; one of its guanidino-NH groups is hydrogen-bonded to the *C2* oxygen of the flavin (1.94 Å), which is 2.58 Å from the 3′ oxygen of the ribityl side chain of FAD, while another guanidino-NH also hydrogen bonds to this 3′ oxygen (2.04 Å) (Figure 2). Hence, for PchF[R474K], it seemed reasonable to speculate that the replacement lysyl residue would also position its positively charged ϵ-ammonium group in close proximity to the *C2* oxygen to mimic the guanidino group of Arg474 in PchF. The necessity of an electropositive environment is supported by our work with apo-PchF-[R474A]. It does not form a covalent bond to FAD in the presence of PchC, nor does it bind FAD in a noncovalent manner with appreciable affinity. It is concluded that the positive charge is also required for noncovalent FAD binding, to aid in maintaining the structural integrity of the FAD binding site.

This is not the first instance of a replacement of this type in an enzyme containing a covalently bound flavin; it was carried out also with trimethylamine dehydrogenase (TMADH; Arg222 replaced) (*31*), which has FMN attached to a cysteinyl residue via the *C6* carbon of the isoalloxazine ring (6-*S*-cysteinyl-FMN). The mechanism for linkage to the 6 position of flavin is essentially the same as that for 8α-carbon tethering (*11*). The level of covalent flavin binding to heterologously expressed wild-type TMADH was low. Only 65% was recovered as apo-enzyme, which could not bind FMN either noncovalenty or covalently. The pure TMADH-[R222K] mutant only had 1.5% of FMN bound, and the remainder was apo-protein, which again, could not bind FMN. Hence, the results were not as definitive for TMADH as are those in the present paper. Here, purified recombinant PchF, PchF[R474K], and PchF[Y384F] each contained a high level of noncovalently bound FAD after purification. The FAD may be removed easily and reinserted quantitatively into the proteins under very mild conditions (*9*, *10*). Further, on addition of PchC to either PchF^{NC} (*9*, *10*) or PchF[R474K]^{NC}, the FAD becomes covalently bound quanitatively.

As predicted, apo-PchF[R474K] was covalently flavinylated when exposed to FAD and PchC but at a reduced rate when compared to apo-PchF. This may be due to a suboptimal orientation of the 8α-methide (the electrophilic center) and/or the Tyr384 phenolate nucleophile (Figure 3) in the former protein that might result from perturbations of the complicated hydrogen-bonding network at the FAD binding site in the vicinity of Arg474 (Figure 2). On the other hand, the slower reaction may be attributable to a lower two-electron $E_{m,7}$ for PchF[R474K]^{NC} (electrophilicity) compared to that for PchF^{NC} (*12*).

In conclusion, the studies of PchF[R474K]^{NC}, PchF-[R474K]^{C}, and PCMH[R474K]^{C} indicate that these mutant proteins retain all of the basic properties of their corresponding wild-type forms. It is particularly important to note that the FAD in PchF[R474K]^{NC} becomes covalently attached when this protein associates with its heteromeric partner, PchC. This supports the proposition that there must be a positively charged environment near the *C2* oxygen of the flavins isoalloxazine ring for covalent flavinylation to occur (see Figure 3). On the other hand, the differences between PchF[R474K]^{NC}, PchF[R474K]^{C}, and PCMH[R474K]^{C} and their wild-type counterparts, in particular their catalytic efficiencies and CT interactions, have provided insights concerning the fundamental principals underlying efficient catalysis by PCMH, as well as for other (flavo)proteins. For example, it was discovered that PCMH not only optimizes the redox properties of covalently bound FAD to facilitate *p*-cresol oxidation, but also the redox properties of this substrate are optimized to make it a better reductant. Further work along these lines is in progress, and this effort should yield further insights into the mechanism of oxidation of this flavocytochrome.

SUPPORTING INFORMATION AVAILABLE

Spectral characterization data, figures, mathematical derivation, and an expanded discussion of the peripheral findings. This material is available free of charge via the Internet at http://pubs.acs.org.

REFERENCES

1. Hopper, D. J, Jones, M. R., and Causer M. J. (1985) Periplasmic location of *p*-cresol methylhydroxylase in *Pseudomonas putida*, *FEBS Lett. 182*, 485−488.

2. Hopper, D. J. (1976) The hydroxylation of *p*-cresol and its conversion to *p*-hydroxybenzaldehyde in *Pseudomonas putida*, *Biochem. Biophys. Res. Commun. 69*, 462−468.
3. McIntire, W. S., Hopper, D. J., and Singer, T. P. (1985) *p*-Cresol methylhydroxylase. Assay and general properties, *Biochem. J. 228*, 325−335.
4. Kim, J., Fuller, J. H., Cecchini, G., and McIntire, W. S. (1994) Cloning, sequencing, and expression of the structural genes for the cytochrome and flavoprotein subunits of *p*-cresol methylhydroxylase from two strains of *Pseudomonas putida*, *J. Bacteriol. 176*, 6349−6361.
5. Mathews, F. S., Chen, Z. W., Bellamy, H. D., and McIntire, W. S. (1991) Three-dimensional structure of *p*-cresol methylhydroxylase (flavocytochrome *c*) from *Pseudomonas putida* at 3.0-Å resolution, *Biochemistry 30*, 238−247.
6. Cunane, L. M., Chen, Z., Shamala, N., Mathews, F. S., Cronin, C. N., and McIntire, W. S. (2000) Structures of the flavocytochrome *p*-cresol methylhydroxylase and its enzyme−substrate complex: Gated substrate entry and proton relays support the proposed catalytic mechanism, *J. Mol. Biol. 295*, 357−374.
7. Koerber, S. C., McIntire, W. S., Bohmont, C., and Singer, T. P. (1985) Resolution of the flavocytochrome *p*-cresol methylhydroxylase into subunits and reconstitution of the enzyme, *Biochemistry 24*, 5276−5280.
8. McIntire, W., Edmondson, D. E., Singer, T. P., and Hopper, D. J. (1980) 8α-*O*-tyrosyl-FAD: a new form of covalently bound flavin from *p*-cresol methylhydroxylase, *J. Biol. Chem. 255*, 6553−6555.
9. Kim, J., Fuller, J. H., Kuusk, V., Cunane, L., Chen, Z.-W., Mathews, F. S., and McIntire, W. S. (1995) The cytochrome subunit is necessary for covalent FAD attachment to the flavoprotein subunit of *p*-cresol methylhydroxylase, *J. Biol. Chem. 270*, 31202−31209.
10. Engst, S., Kuusk, V., Efimov, I., Cronin, C. N., and McIntire, W. S. (1999) Properties of *p*-cresol methylhydroxylase flavoprotein overproduced by *Escherichia coli*, *Biochemistry 38*, 16620−16628.
11. Mewies, M., McIntire, W. S., and Scrutton, N. S. (1998) Covalent attachment of flavin adenine dinucleotide (FAD) and flavin mononucleotide (FMN) to enzymes: the current state of affairs, *Protein Sci. 7*, 7−20.
12. Efimov, I., Cronin C., and McIntire W. S. (2001) Effects of noncovalent and covalent FAD binding on the redox and catalytic properties of *p*-cresol methylhydroxylase, *Biochemistry 40*, 2155−2166.
13. Fraaije, M. W., and Mattevi, A. (2000) Flavoenzymes: diverse catalysts with recurrent features, *Trends Biochem. Sci. 25*, 126−132.
14. Deng, W. P., and Nickoloff, J. A. (1992) Site-directed mutagenesis of virtually any plasmid by eliminating a unique site, *Anal. Biochem. 200*, 81−88.
15. Cronin, C. N. (1997) cDNA cloning, recombinant expression, and site-directed mutagenesis of bovine liver carnitine octanoyltransferase. Arg505 binds the carboxylate group of carnitine, *Eur. J. Biochem. 247*, 1029−1037.
16. McIntire, W. S., and Singer, T. P. (1982) Resolution of *p*-cresol methylhydroxylase into catalytically active subunits and reconstitution of the flavocytochrome, *FEBS Lett. 143*, 316−318.
17. Koerber, S. C., Hopper, D. J., McIntire, W. S., and Singer, T. P. (1985) Formation and properties of flavoprotein-cytochrome hybrids by recombination of subunits from different species, *Biochem. J. 231*, 383−387.
18. Cronin, C. N., and McIntire, W. S. (2000) Heterologous expression in *Pseudomonas aeruginosa* and purification of the 9.2-kDa c-type cytochrome subunit of *p*-cresol methylhydroxylase, *Protein Expression Purif. 19*, 74−83.
19. Pace, C. N., Vajdos, F., Fee, L., Grimsley, G., and Gray, T. (1995)- How to measure and predict the molar absorption coefficient of a protein, *Protein Sci. 4*, 2411−2423.
20. Edmondson, D. E., and Singer, T. P. (1973) Oxidation−reduction properties of the 8α-substituted flavins, *J. Biol. Chem. 248*, 8144−8149.
21. Massey, V. (1991) A simple method for the determination of redox potentials, in *Flavins and Flavoproteins 1990* (Curti, B., Ronchi, S., and Zanetti, G., Eds.) pp 59−66, Walter de Gruyter, New York.
22. McIntire, W. S., Hopper, D. J., and Singer, T. P. (1987) Steady-state and stopped-flow kinetic measurements of the primary deuterium isotope effect in the reaction catalyzed by *p*-cresol methylhydroxylase, *Biochemistry 26*, 4107−4117.
23. Stewart, R. C., and Massey V. (1985) Potentiometric studies of native and flavin-substituted Old Yellow Enzyme, *J. Biol. Chem. 260*, 13639−13647.
24. Clark, W. S. (1972) *Oxidation−Reduction Potentials of Organic Systems*, Chapter 7, pp 184−203, Robert E. Krieger Publishing Co., Huntington, NY.
25. McIntire, W. S., Everhart, E. T., Craig, J. C., and Kuusk, V. (1999) A new procedure for deconvolution of inter-/intramolecular intrinsic primary and α-secondary deuterium isotope effects from enzyme steady-state kinetic data, *J. Am. Chem. Soc. 121*, 5865−5880.
26. Leffler, J. E., and Grunwald, E. (1963) *Rates and Equilibria of Organic Reactions*, p 157, Wiley & Sons, New York.
27. Connors, K. A. (1990) *Chemical Kinetics. The Study of Reaction Rates in Solution*, pp 220−229, VCH Publishers, New York.
28. Abramovitz, A. S., and Massey, V. (1976) Interaction of phenols with Old Yellow Enzyme. Physical evidence for charge-transfer complexes, *J. Biol. Chem. 251*, 5327−5336.
29. Hopkins, N., and Stanley, R. J. (2003) Measurement of the electronic properties of the flavoprotein old yellow enzyme (OYE) and the OYE:*p*-Cl phenol charge-transfer complex using Stark spectroscopy, *Biochemistry 42*, 991−999.
30. Edmondson, D. E., and Newton-Vinson, P. (2001) The covalent FAD of monoamine oxidase: structural and functional role and mechanism of the flavinylation reaction, *Antioxid. Redox Signaling* 3, 789−806.
31. Mewies, M., Packman, L. C., Mathews, F. S., and Scrutton, N. S. (1996) Flavinylation in wild-type trimethylamine dehydrogenase and differentially charged mutant enzymes: a study of the protein environment around the N1 of the flavin isoalloxazine, *Biochem. J. 317*, 267−272.

BI035772X